Electronic Supplementary Material (ESI) for Catalysis Science & Technology.

Supporting Information

Formation of graphene encapsulated cobalt–iron phosphide nanoneedles as an attractive electrocatalyst for overall water splitting

Zeinab Tahmasebi, Akbar Mohammadi Zardkhoshoui, and Saied Saeed Hosseiny Davarani*

Department of Chemistry, Shahid Beheshti University, G. C., 1983963113, Evin, Tehran, Iran. Corresponding author: *Tel: +98 21 22431661; Fax: +98 21 22431661; E-mail: ss-hosseiny@sbu.ac.ir (S.S.H. Davarani).

HER performance in H_2SO_4 and PBS solution

The HER performance of CFP-G@NF follows a similar pattern as in the KOH medium. The LSV curves in an acidic electrolyte (Fig. S6A) show that CFP-G@NF demonstrates the highest HER performance with the smallest overpotentials of 64 mV to acquire a current density of 10 mA/cm^2 compared with CoP@NF (185 mV), CoFeP@NF (101 mV), and bare NF electrodes. As expected, the bare NF electrode without active materials reveals an insignificant response. In comparison to other reports, the CFP-G@NF catalyst illustrated superior catalytic performance, further revealing its good properties toward HER in an acidic medium (Fig. S6B).[1-7] Besides, the obtained Tafel slope of CFP-G@NF (65 mV/dec) reflected in Fig. S6C is smaller than that of CoFe-P@NF (76 mV/dec), and CoP@NF (91 mV/dec), illustrating the superb electrocatalytic activity of CFP-G@NF in H_2SO_4 medium. The enhanced performance of CFP-G@NF toward HER in the acidic electrolyte was also revealed using its desirable stability. Hence, the stability of CFP-G@NF for HER was examined in detail by CV and chronopotentiometry techniques. As evidenced in Fig. S6D, after 2000 uninterrupted CV cycles at 100 mV s^{-1}, the polarization plot of the CFP-G@NF is essentially unchanged, which implies that the CFP-G@NF possesses reasonable stability. Also, the durability of CFP-G@NF was also evaluated using chronopotentiometry at 10 mA/cm^2 in a period of 12 h. From Fig. S6E, it can be discovered that the CFP-G@NF catalyst indicates remarkable stability, displaying its satisfactory stability. We then tested HER performance of the CFP-G@NF in neutral solution (1 M PBS solution) to identify the good HER performance of our catalyst in a wide pH range. Fig. S7A reflects the polarization plots of the investigated CFP-G@NF electrode, together with the CoFe-P@NF, CoP@NF, and original NF electrodes in neutral media. Obviously, the original NF is not a favorable HER electrocatalyst. In stark contrast, the CFP-G@NF depicts satisfactory electrochemical activity yielding a current density of 10 mA/cm^2 at 161 mV, demonstrating that its performance is better that of CoFeP@NF (216 mV) and CoP@NF (327 mV). Particularly, the HER performance of the CFP-G@NF electrode is better than several of the reported materials as depicted in Fig. S7B.[3,6-10] Fig. S7C represents the relevant Tafel curves of as-made catalysts. The Tafel slope of 98 mV/dec obtained for CFP-G@NF is lower than that of CoFe-P@NF (160 mV/dec) and CoP@NF (168 mV/dec) in 1 M PBS. We also explored the stability of CFP-G@NF by CV analysis for 2000 cycles at 100 mV s^{-1}. After 2000 cycles, the shape of the LSV plot has no evident change as compared to the initial cycle (Fig. S7D). On the other hand, the durability of CFP-G@NF was evaluated through chronopotentiometry at 10 mA/cm^2 for 12 h (Fig. S7E). It is noteworthy that the potential response of CFP-G@NF has no drastic decline with time, illustrating the distinguished durability of CFP-G@NF in a neutral environment.

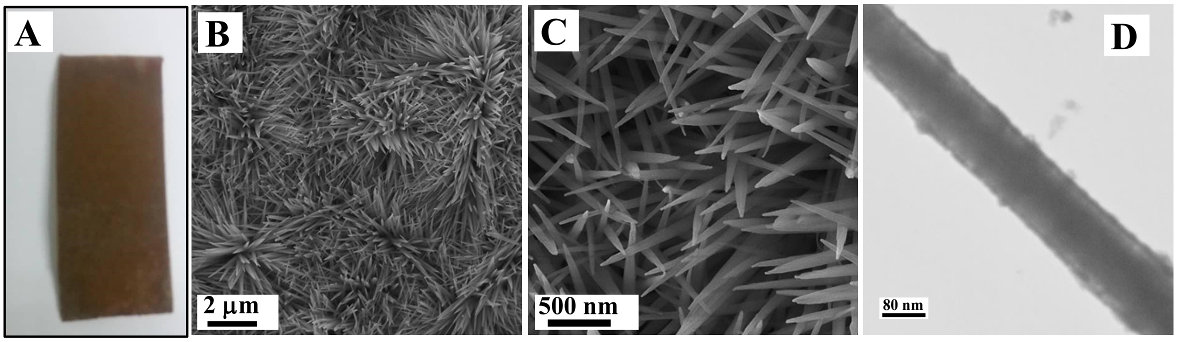

Fig. S1 (A) Photograph of the CoFe-LDH@NF. (B and C) FE-SEM images of the CoFe-LDH@NF. (D) TEM image of the CoFe-LDH sample.

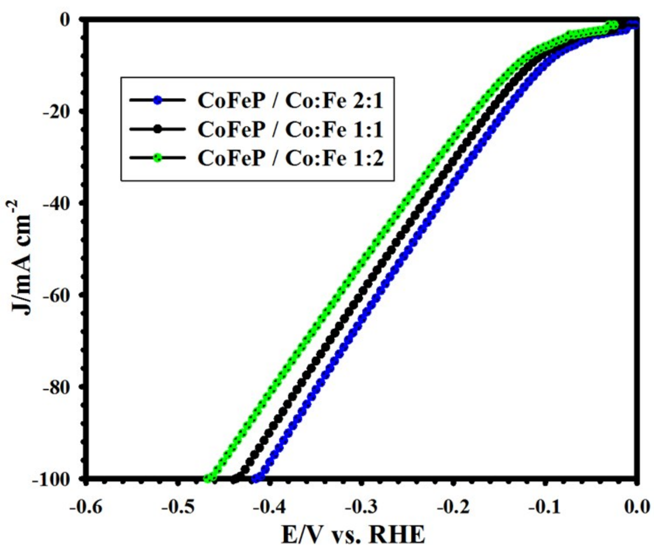

Fig. S2 Polarization LSV curves of the CoFeP with several stoichiometric ratios of the Co: Fe (2:1, 1:1, and 1:2) for HER in 1M KOH.

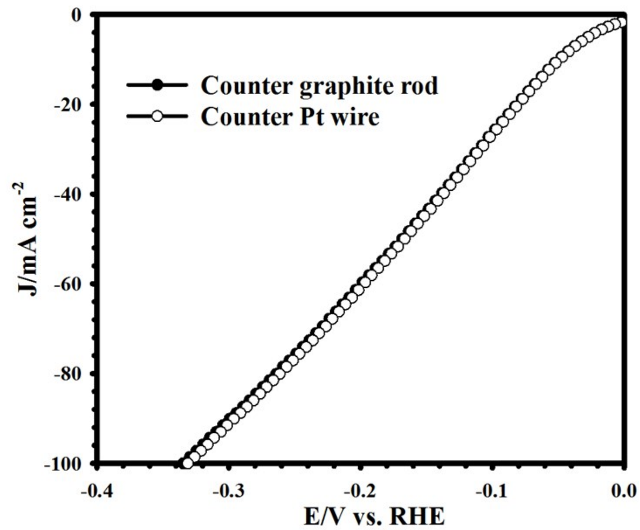

Fig. S3. The comparative LSV curves of CFP-G@NF electrode with Pt wire and graphite rod.

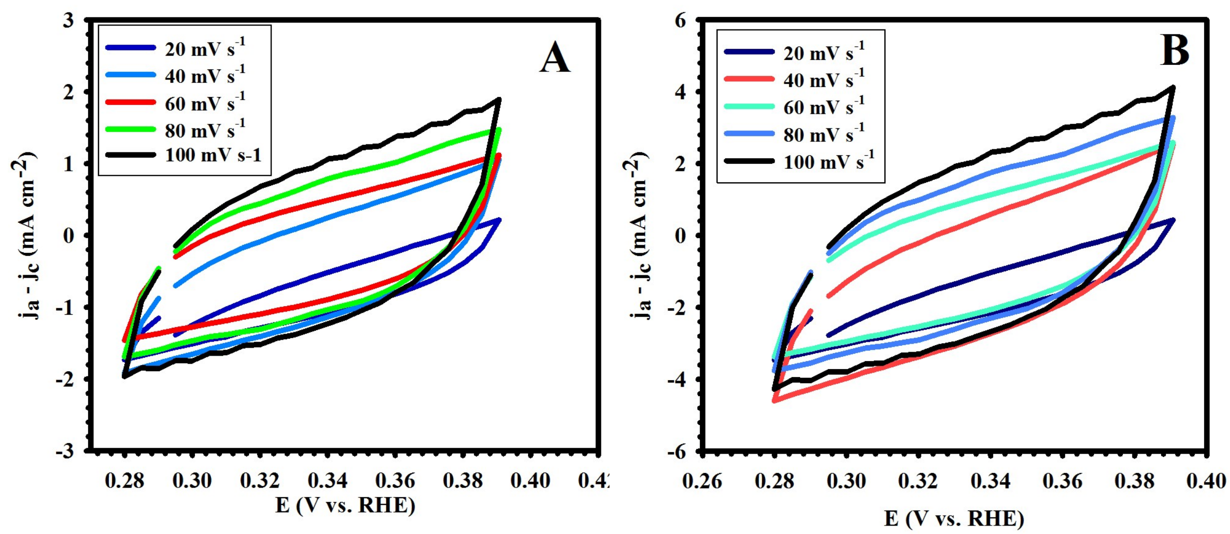

Fig. S4 (A) CV curves of the CoFe-P@NF at various scan rates. (B) CV curves of the CFP-G@NF at various scan rates.

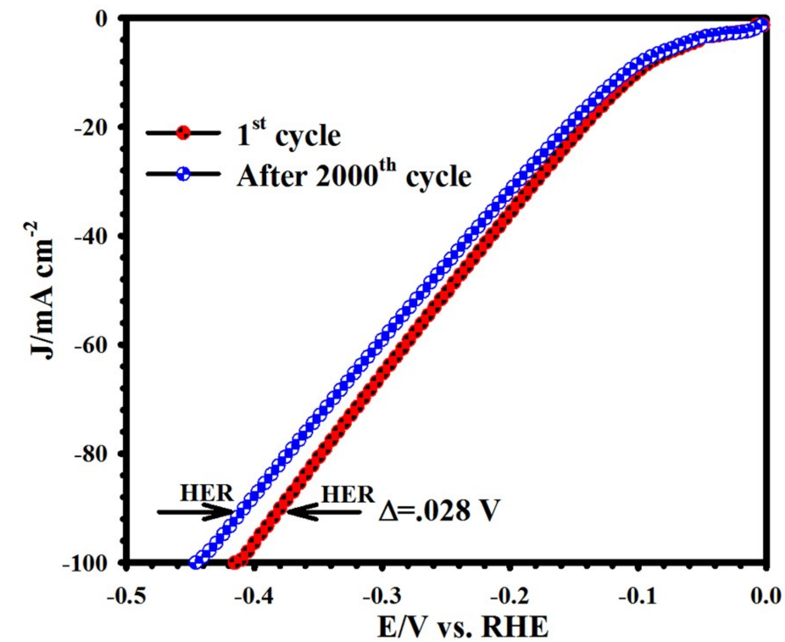

Fig. S5 Polarization curves for the CFP@NF before and after 2000th CV cycles for HER in 1 M KOH.

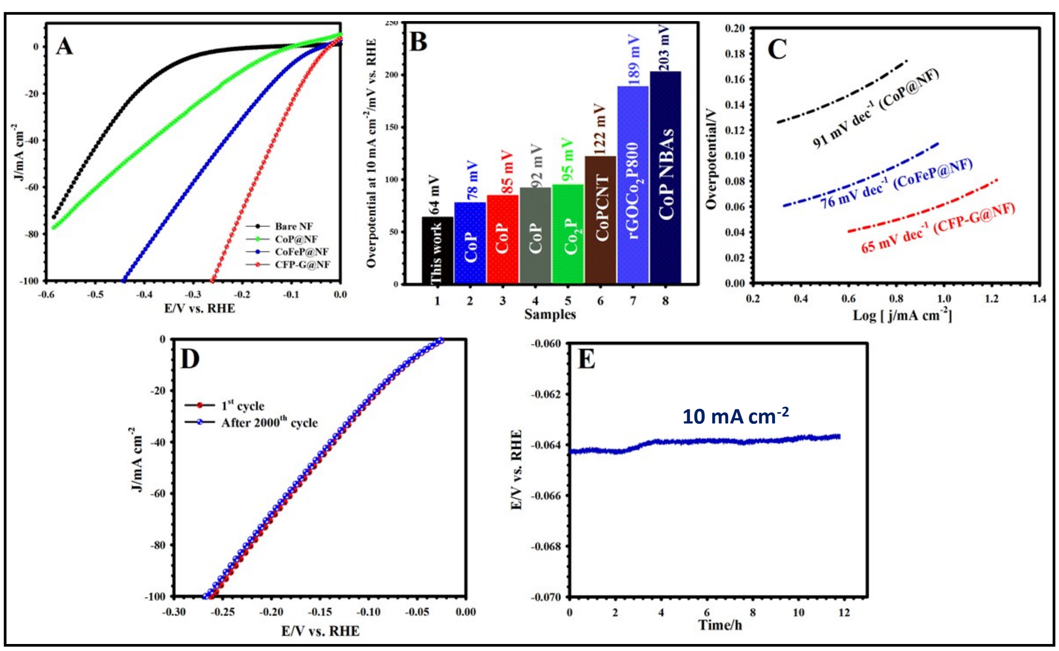

Fig. S6 (A) HER polarization plots of CFP-G@NF, CoFe-P@NF, CoP@NF, and bare NF in .5 M H_2SO_4 electrolyte. (B) Comparison of η at 10 mA/cm^2 between CFP-G@NF and previous reports in acidic medium. (C) Related Tafel slops for CoP@NF, CoFe-P@NF, and CFP-G@NF. (D) The polarization plot for the CFP-G@NF before and after 2000th CV cycles in .5 M H_2SO_4. (E) chronopotentiometric measurement of CFP-G@NF toward HER at 10 mA/cm^2 for 12 h in .5 M H_2SO_4.

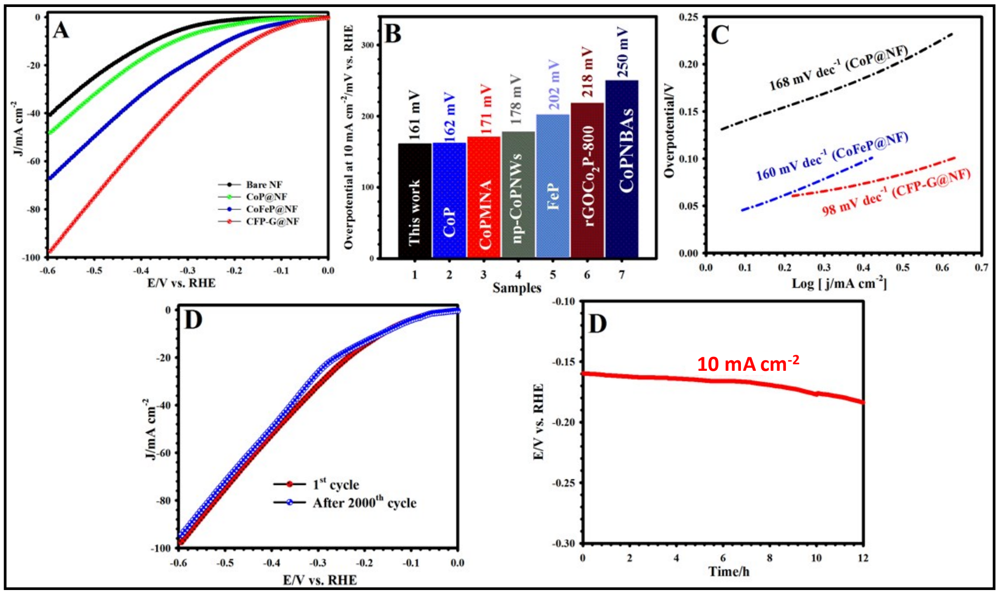

Fig. S7 (A) LSV curves of the CFP-G@NF, CoFe-P@NF, CoP@NF, and bare NF for HER in 1 M PBS. (B) Comparison of η at 10 mA/cm^2 between CFP-G@NF and previous reports in neutral medium. (C) Tafel plots of CFP-G@NF, CoFe-P@NF, and CoP@NF electrocatalysts in neutral medium. (D) The LSV plot for the CFP-G@NF before and after 2000th CV cycles in 1 M PBS. (E) chronopotentiometric measurement of CFP-G@NF toward HER at 10 mA/cm^2 for 12 h in 1 M PBS.

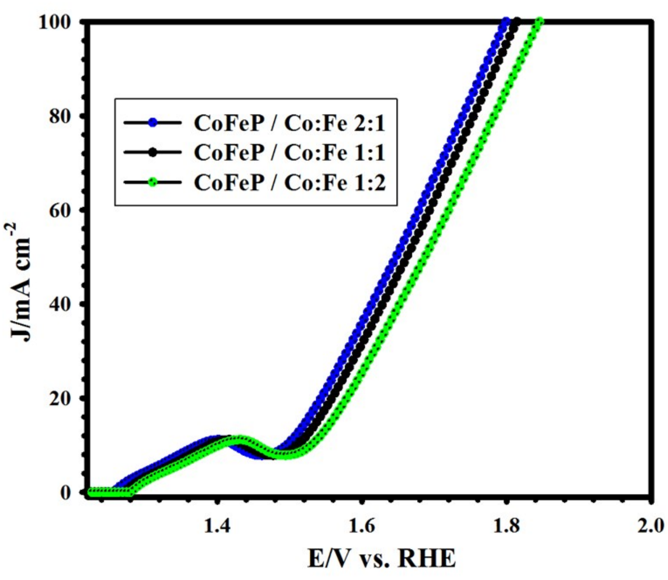

Fig. S8 Polarization LSV curves of the CoFeP with several stoichiometric ratios of the Co: Fe (2:1, 1:1, and 1:2) for OER in 1M KOH.

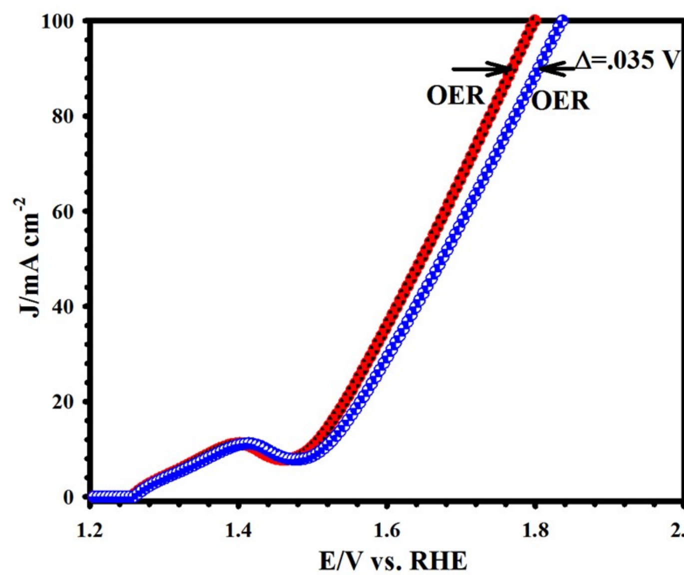

Fig. S9 Polarization curves for the CFP@NF before and after 2000th CV cycles for OER in 1 M KOH.

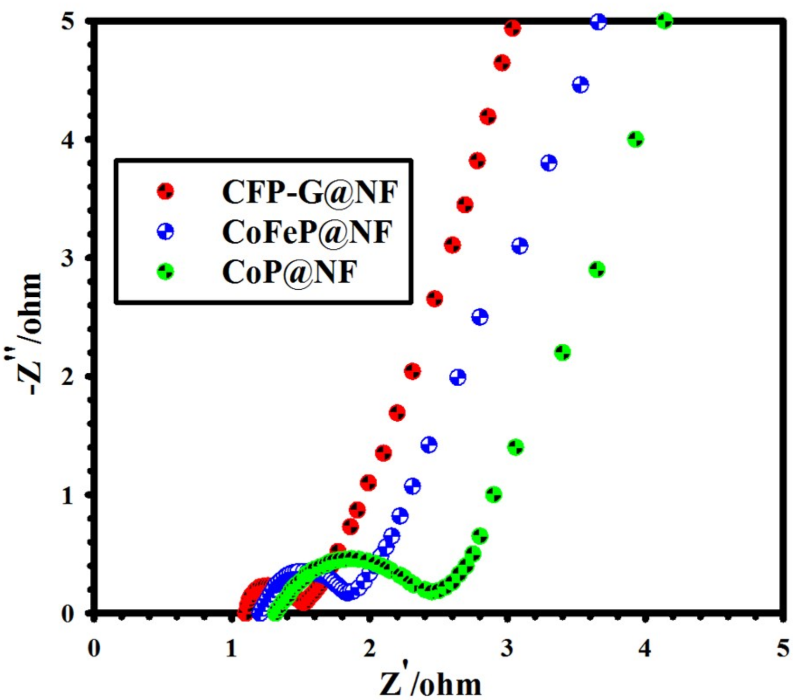

Fig. S10 EIS measurements of CoP@NF, CoFe-P@NF, and CFP-G@NF electrodes.

Table S1. Comparison of the catalytic performance of the CFP-G@NF electrode with other previously reported electrodes.

Catalyst	Current collector	Electrolyte	Catalyst morphology	Overpotential of HER for J=10 mA cm^{-2}(mV)	Overpotential of OER for J=10 mA cm^{-2}(mV)	Ref
NiCoP	Nickel foam	1 M KOH	Nanoleaves	98	-	11
NiCoFeP@NiCoP	Nickel foam	1 M KOH	Pagoda-like	77	-	12
ip-CoP	Carbon fiber	1 M KOH	Nanowire	76	300	13
CoP	Carbon Cloth	1 M KOH	Nanoneedle	95	281	14
NiSe@CoP	Nickel foam	1 M KOH	Core-Shell Nanowires	91	-	15
NiCoP	Nickel foam	1 M KOH	Nanowire	104	277	16
Ni_2P	Nickel foam	1 M KOH	Nanosheet	102		17
Cu-CoP	Carbon cloth	1 M KOH	Nanorod	81		18
$Co_{5.0}Mo_1P$/NiFe-LDH	Nickel foam	1 M KOH	Nanosheet	98.9	-	19
V doped CoP	Carbon cloth	1 M KOH	Nanowall	87	-	20
CFP-G	Nickel foam	1 M KOH	graphene encapsulated nanoneedles	71	260	This work

References:

1 J. Huang, Y. Li, Y. Xia, J. Zhu, Q. Yi, H. Wang, J. Xiong, Y. Sun and G. Zou, *Nano Res* 2017, **10**, 1010-1020.

2 F. H. Saadi, A. I. Carim, E. Verlage, J. C. Hemminger, N. S. Lewis and M. P. Soriaga, *J. Phys. Chem. C* 2014, **118**, 29294-29300.

3 X. Lu, X. Yan, S. Devaramani, D. Qin, J. Chen, D. Shan and Q. Ma, *New J. Chem*. 2017, **41**, 2436-2442.

4 J. F. Callejas, C. G. Read, E. J. Popczun, J. M. McEnaney and R. E. Schaak, *Chem. Mater*. 2015, **27**, 3769-3774.

5 Q. Liu, J. Tian, W. Cui, P. Jiang, N. Cheng, A. M. Asiri and X. Sun, *Angew. Chem. Int. Ed*. 2014, **53**, 1-6.

6 X. Zhao, Y. Fan, H. Wang, C. Gao, Z. Liu, B. Li, Z. Peng, J. H. Yang and B. Liu, *ACS Omega* 2020, **5**, 6516-6522.

7 Z. Niu, J. Jiang and L. Ai, *Electrochem. Commun.* 2015, **56**, 56-60.

8 Y. P. Zhu, Y. P. Liu, T. Z. Ren and Z. Y. Yuan, *Adv. Funct. Mater*. 2015, **25**, 7337-7347.

9 S. Gu, H. Du, A. M. Asiri, X. Sun and C. Li, *Phys. Chem. Chem. Phys*. 2014, **16**, 16909-16913.

10 Y. Liang, Q. Liu, A. M. Asiri, X. Sun and Y. Luo, *ACS Catal*. 2014, **4**, 4065-4069.

11 L. Chen, Y. Song, Y. Liu, L. Xu, J. Qin, Y. Lei and Y. Tang, *J. Energy Chem* 2020, **50**, 395-401.

12 G. Yan, H. Tan, Y. Wang and Y. Li, *Appl. Surf. Sci.* 2019, **489**, 519-527.

13. S. Zhang, T. Xiong, X. Tang, Q. Ma, F. Hu and Y. Mi, *Appl. Surf. Sci*. 2019, **481**, 1524–1531.

14. P. Wang, F. Song, R. Amal, Y. H. Ng and X. Hu, *ChemSusChem* 2016, **9**, 472-477.

15. Y. Xu, C. Yuan, Z. Liu and X. Chen, *Catal. Sci. Technol*. 2018, **8**, 128-133.

16. J. Li, G. Wei, Y. Zhu, Y. Xi, X. Pan, Y. JI, Igor. V. Zatovsky and W. Han, *J. Mater. Chem. A*, 2017, **5**, 14828-14837.

17. J. Ren, Z. Hu, C. Chen, Y. Liu and Z. Yuan, *J. Energy Chem.* 2017, **26**, 1196-1202.

18. L. Wen, Y. Sun, C. Zhang, J. Yu, X. Li, X. Lyu, W. Cai and Y. Li, *ACS Appl. Energy Mater*. 2018, **1**, 3835–3842.

19. W. Mai, Q. Cui, Z. Zhang, K. Zhang, G. Li, L. Tian and W. Hu, *ACS Appl. Energy Mater*. 2020, **3**, 8075–8085.

20. X. Wang, Y. Chen, J. He, B. Yu, B. Wang, X. Zhang, W. Li, M. Ramadoss, W. Zhang and D. Yang, *ACS Appl. Energy Mater*. 2020, **3**, 1027–1035.